On the Tensor Glueball Content of Soft Pomeron*

ZHOU Li-Juan[1;1)] MA Wei-Xing[1,2] L.C.Liu[3]

1(Department of Information and Computing Science, Guang xi University of Technology, Liuzhou 545006, China)

2(Institute of High Energy Physics, CAS, Beijing 100039, China)

3(T-16, Theoretical Division, Los Alamos National Laboratory, Los Alamos, NM 87545, USA)

Abstract We study the gluonic content of the pomeron through relating the pomeron trajectory to the observed $I^GJ^{PC}=0^+2^{++}$ isoscalar tensor mesons. Four of these mesons satisfy the spin-mass relation of the pomeron. These pomeronian candidates may be hybrid states. One of them, the $f_2(2220)$ meson, can have a predominant glueball component. We address the unsettled experimental situation about the width of this meson and give a theoretical lower bound for it. We also show why this meson may not be seen in $\bar{p}p$ experiments.

Key words pomeron, glueballs, mesons

1 Introduction

Before the advent of the quantum chromodynamics (QCD) field theory, Regge theory was successfully used in describing and predicting hadron-hadron elastic scattering and diffractive dissociation[1,2]. Although Regge theory is not a field theory, it is based upon a set of postulates (or axioms) about the S-matrix, which is believed to govern the strong interaction physics. Consequently, the Regge theory can not be completely disconnected from QCD. In Regge theory, mesons and baryons are organized into families of trajectory (the Regge trajectories or Reggeons). These trajectories play an important role in hadronic dynamics. The most tantalizing prediction of the theory is that when the interaction energy becomes very large only one trajectory contributes to hadron-hadron elastic scattering. This unique trajectory is called the pomeron trajectory or pomeron, named in honor of physicist I. Y. Pomeranchuk[3]. The members of the pomeron trajectory all have the quantum numbers of a vacuum except their spins.

Although no particles that fit the pomeron properties were observed during the heydays of the Regge theory, many new particles have been discovered thanks to a new generation of accelerators. Some of these particles may be the glueballs predicted only by the QCD theory. As a result of this progress, there is a surge of interests in understanding the success of the Regge theory through connecting glueballs with the pomeron. Because glueballs are bound states of the gluons, they can only be understood in terms of nonperturbative QCD. An establishment of the pomeron-glueball link could aid our understanding of nonperturbative QCD.

In section 2, we recapitulate the main results of the Regge theory on the pomeron. In section 3, we discuss the gluonic content of the pomeron. We show in section 4 the connection between pomeron and tensor mesons with a focus on the $f_2(2220)/\xi$ meson because of the reported flavor-symmetry decay and the unsettled experimental situation. We give a lower bound for the width of ξ, with which the seemingly opposing results given by different experiments can be explained. The conclusions are given in section 5.

Received 10 March 2003

* Supported by National Natural Science Foundation of China (10247004, 10075081)

1) E-mail: MAWX@mail.ihep.ac.cn

2 Regge theory and pomeron

Unlike QCD field theory, the Regge theory does not involve gauge particles. Instead, it explores the consequences of a set of fundamental postulates of the S-matrix; in particular, the Lorentz invariance, the unitarity, and the analyticity of the S-matrix. The Regge theory was motivated by the experimental observation that at high energies the hadron-hadron (hh) elastic scattering and diffractive dissociation are mainly diffractive. Because exchanging a particle in t-channel will give rise to a forward-peaking, diffractive amplitude in the s-channel, the Regge theory conjectures that the high-energy hadronic dynamics is driven by t-channel exchanges.

There is, however, an important difference between the Regge theory and the meson-exchange model used in medium-energy physics. It can be shown that the exchange of a particle of spin J in the t-channel will necessarily lead to a total cross section $\sigma^{\rm tot}(s) \approx s^{J-1}$, which diverges with s for $J > 1$. Hence, simple particle-exchange models will lead to divergent energy-dependent cross sections, which have to be cured by introducing ad-hoc energy-cutoff form factors. Regge theory overcame this difficulty by not using particle exchanges but by using trajectory exchanges with each trajectory carrying a running spin $\alpha(t)$, which is a complex-valued function of the exchanged 4-momentum t. The connection of a Regge trajectory, $\alpha(t)$, to a physical particle having mass m and spin J is that $J = \mathrm{Re}[\alpha(t = m^2)]$. In other words, a Regge trajectory or a Reggeon is a family of reggeized particles constrained on a spin trajectory $\alpha(t)$.

As a result of trajectory exchange, the Regge theory gives $\sigma^{\rm tot} \approx s^{\alpha(0)-1}$. Because all the trajectories associated with the then known particles[2] have $\alpha(0) < 1$, the cross section no longer diverges. In fact, this last inequality implies that the contribution of a given trajectory will die off at very high energies. However, experimental total cross sections do not vanish asymptotically[4]. Instead, they rise slowly as s increases. The high-energy total cross sections of the pp, $\bar{\rm p}$ p, π^+ p, π^- p reactions are found to follow the energy dependence[5]

$$\sigma_{\rm tot} = As^{0.0808} + Bs^{-0.4525}\,(mb), \qquad (1)$$

where A and B are constants. The appearance of a universal exponent 0.0808 indicates unequivocally that if one attributes this mild rise of cross sections to the exchange of a single Regge trajectory, then this trajectory has $\alpha(0) \approx 1.08$.

The s-dependence of the cross sections is shown in Fig.1 where at high energies $\sigma(\mathrm{pp}) = \sigma(\bar{\rm p}\mathrm{p})$ and $\sigma(\pi^+\mathrm{p}) = \sigma(\pi^-\mathrm{p})$. The equality $\sigma(\mathrm{hp}) = \sigma(\bar{\rm h}\,\mathrm{p})$ at very high energies was foreseen by Pomeranchuk[3]. In order to account for it, this Regge trajectory must carry the quantum numbers of vacuum, except its spins. In other words, it has $B = Q = S = I = 0$ and $P = G = C = +$ but with spin J given by $\alpha(t)$. This unique trajectory was named the pomeron trajectory (or pomeron).

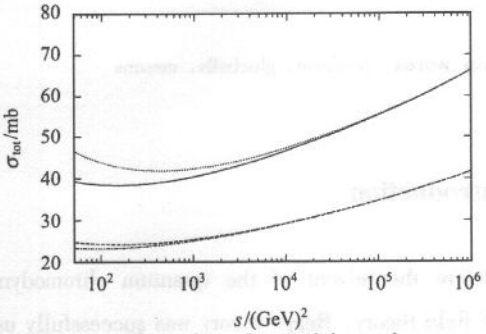

Fig.1. The s-dependence of the total cross sections for various reactions.

Although the Regge trajectory $\alpha(t)$ can be a nonlinear function of t, it can be well approximated by a linear function at low ts. For the purpose of studying pomeron, it suffices to use the form

$$\alpha(t) = 1.08 + \alpha' t. \qquad (2)$$

In contrary to $\alpha(0)$, the value of the slope α' is less unanimous. The most extensively quoted value of $\alpha' = 0.25 \pm 0.02$ was first given in Ref.[6], resulted from fitting the slope of the pp elastic differential cross sections at small momentum transfers. There are two other methods that have been used for determining the α'. One method used an effective trajectory approach (§6.8e of Ref.[2]) which gave[7] an $\alpha' = 0.20 \pm 0.01$. The other[8] used the relation[9]

$$\sigma_{\rm tot}^2(s)/\sigma_{\rm el}(s) = 16\pi(b + 2\alpha' \ln(s)),$$

with b being the slope of the experimental elastic diffraction peak. The p$\bar{\rm p}$ total and elastic cross sections then gave[8] an $\alpha' = 0.20 \pm 0.02$. Hence, the last two methods gave the same result.

One should note, however, that the analysis of Ref.[6] that led to $\alpha' = 0.25$ is model-dependent. More pre-

cisely, the theoretical formula employed for fitting the data was based on a phenomenological quark model and on valence quark counting rule. Consequently, it is not possible to know the systematic uncertainty of the α', arising from using such a theoretical model. In contrast, the methods of Refs.[2] and [8] are model independent. In particular, in spite of the use of very different data sets, these two different methods gave the same α'. For this reason, the value of $\alpha' = 0.20$ should be chosen.

In Fig.2 we plot the pomeron trajectory zone defined by different values of α'. We also plot, in ascending mass order, the isoscalar tensor resonances $f_2'(1525)$, $f_2(1565)$, $f_2(1640)$, $f_2(1810)$, $f_2(1950)$, $f_2(2010)$, $f_2(2150)$, $f_2(2220)$, $f_2(2300)$, $f_2(2340)$, As ws can see, the $f_2(2010)$, $f_2(2150)$, $f_2(2220)$ are inside the zone bordered by the solid lines. The $f_2(1950)$ is marginal because it is inside the zone only when the higher value of 0.25 (the chain-dotted line) is used.

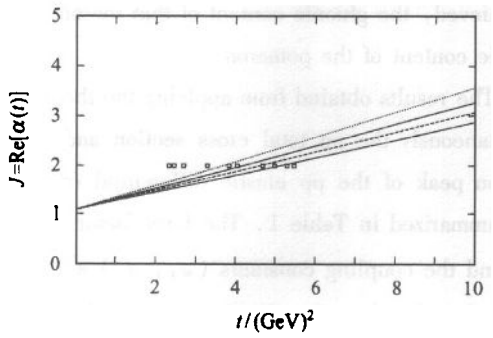

Fig.2. Zone of pomeron trajectory. The threshold of $p\bar{p}$ is at $t = 3.52\ (GeV)^2$.

To this end, we caution that in the literature two kinds of pomerons, hard and soft, have been discussed. The hard pomeron is associated with large momentum transfer. Recent experimental data on large rapidity gap events at HERA[10] gave some evidence for the existence of large Q^2, hard pomeron. It is not the original or the soft pomeron conjectured in Regge theory, the latter is associated with small Q^2. The four tensor resonances mentioned in the previous paragraph are, therefore, the candidates for the soft pomeron. In terms of QCD, the hard pomeron is in the perturbative (pQCD) regime while the soft pomeron must be studied with nonperturbative method. The evolution from the hard to soft pomeron or vice versa is still an unresolved problem. There are many studies of diffractive processes using hard or semi-hard pomeron models[5,11]. We shall not discuss these models and will concentrate on the soft Pomeron.

3 Gluonic content of the pomeron

In QCD, the simplest model for vacuum exchange with properties similar to that of the pomeron is two interacting gluons. This was emphasized by Nachtmann[12], who stated that the two-gluon system has all the properties that a pomeron should possess. The idea of modeling the pomeron with two gluons was originated by Low[13]. The model was further developed by Nussinov[14] who considered more than two gluons. Subsequent and more sophisticated considerations led to the development of BKFL[15] and DGLAP[16] equations. All these models use pQCD and all gave an $\alpha(0) \gg 1$. These studies indicate, therefore, that models involving gluons but not bound gluons cannot describe the soft Pomeron. Consequently, if gluons are the constitutents of the soft pomeron, they must be in a bound state.

The existence of bound states of gluons (the glueballs) is a consequence of self-coupling of gluons in QCD. Lattice calculations and other theoretical models[17,18] have predicted that the lightest glueballs have $J^{PC} = 0^{++}$ (scalar glueball) and 2^{++} (tensor glueball).

Although scalar glueballs have been studied extensively[19,20], they cannot be the soft pomeron because spin = 0 is ruled out by Eq.(2). Moreover, Levin noted[21] that the process due to exchanging scalar particle is not diffractive and becomes less important as energy increases. From the discussion given after Eq.(2), the lightest soft pomeron must have spin = 2. Fig.2 indicates that four $J = 2$ isoscalar tensor resonances in the 2 GeV mass region are compatible with the pomeron trajectory. Can one of them be a tensor glueball?

Calculated glueball spectra predict[17,18,22] that the lightest 2^{++} tensor glueball has a mass about 2.2 ± 0.3GeV. Because in lattice calculations the quark masses are taken to be infinite and the $q\bar{q}$ loops are neglected, the mixing of $q\bar{q}$ and glueball states can not occur in those calculations. However, the existence of a 2^{++} tensor glueball in the 2 GeV mass region is also predicted by other theoretical models[23,24]. In addition, a mass-

equation analysis of all the observed isoscalar tensor states has indicated[25] that while $f_2'(1525)$ and $f_2(1640)$ are definitely quarkoniums, the tensor states of larger masses can be $q\bar{q}$-gluons hybrids. The mass equation also has a solution corresponding to $f_2(2220)$ being almost a tensor glueball.

In summary, the soft pomeron can not be unbound gluons or scalar glueballs. The pomeronian candidates have $I^G(J^{PC}) = 0^+(2^{++})$ and a mass in the 2 GeV region. Some analysis suggests that they are hybrid states and one of them, the $f_2(2220)$, may be a tensor glueball.

4 $f_2(2220)/\xi$ meson

In 1986 the MARK Ⅲ collaboration[26] at SLAC observed a narrow resonance, named ξ, in the decay of J/ψ to K_sK_s and K^+K^- channels. It was reported that $M_\xi = 2230 \pm 15$MeV and $\Gamma_\xi = 18^{+23}_{-15} \pm 10$ and $26^{+26}_{-16} \pm 7$MeV respectively, and that $J^{PC} = (\text{even})^{++}$. At the same time, Alde et al. also observed[27] a broad enhancement ($\Gamma \leqslant 150$MeV) at $M = 2220$MeV in the reaction $\pi^- p \to nX$, $X \to \eta\eta'$. The ξ was also seen[28] in $K_s^0K_s^0$ and in the WA91 collaboration[29] at CERN. However, it was not seen in Υ decays and in inclusive B decays. In 1996, BES collaboration[30] reported the observation of $\xi(2230)$ in the radiative decay of the J/ψ to $\bar{p}p$, K^+K^-, $K_s^0K_s^0$, $\pi^+\pi^-$ channels. The data also suggest a spin $J = 2$ or 4. However, the $\xi(2230)$ was not seen in experiments[31] $\bar{p}p \to K^+K^-$, K_sK_s, $\phi\phi$, $\pi^+\pi^-$. In our opinion, these seemingly contradictory experimental results does not necessarily rule out the existence of ξ. We will come back to this point toward the end of this section. In the following discussion we will use interchangeably the notations $f_2(2220)$ and ξ.

Because the BES collaboration observed ξ in the $J/\psi \to \gamma\xi$, $\xi \to pp$ reaction and because the $\bar{p}p$ channel is related to the pp channel by crossing symmetry, it is of value to investigate contributions by ξ to high-energy pp scattering in the framework of Regge theory. In particular, because pp elastic scattering is a diffractive process[32] in which no quantum numbers are exchanged between the colliding particles, it is an ideal place for investigating the pomeron. If the Regge-exchange of a tensor meson can describe the observed pp elastic scattering as does the pomeron, then it would be a strong indication that meson is a pomeron.

We have carried out such analysis in Ref.[33]. The original analysis was done for the ξ, we now extend it to all f_2 mesons of interest. Although the Regge analysis alone is not sufficient to uniquely determine which tensor state is the pomeron, as we shall see, it gives a definite prediction on the partial decay width $\Gamma_{f_2 \to pp}$ which can be used to analyze experiments to pin down the pomeron. Once the identification of the tensor meson to the pomeron is achieved, the gluonic content of that meson will be the gluonic content of the pomeron.

The results obtaind from applying the theory to fitting simultaneously the pp total cross section and to the diffraction peak of the pp elastic differential cross sections are summarized in Table 1. The form factor ranges (λ_s, λ_t) and the coupling constants (g_1, g_3) are the results of the fit. On the other hand, the partial decay widths $\Gamma_{f_2 \to pp}$ are theoretical predictions based on the fit (see Appendix).

As mentioned at the beginning of this section, there are currently opposing experimental results about the existence of the $f_2(2220)/\xi$ meson. In particular, this resonance was not seen in $\bar{p}p$ experiments, which seems to contradict the results reported in Ref.[30]. We believe that the partial decay width given by our analysis can shed lights on how to understand the unsettled experimental situation.

Table 1. Predicted partial decay widths to the $p\bar{p}$ channel from the pp scattering at $\sqrt{s} = 53$ and 62GeV.

Mesons	$\sqrt{s}$/GeV	λ_s/GeV	λ_t/GeV	g_1	g_3	$\Gamma_{f_2 \to p\bar{p}}$/MeV
$f_2(2220)/\xi$	53	0.65—0.67	3.79—3.82	1.70—1.72	0.00—0.02	1.94—1.99
	62	0.66—0.68	3.74—3.79	1.67—1.70	0.00—0.01	1.88—1.94
$f_2(2150)$	53	0.66	3.88—3.99	1.53—1.56	0.00—0.04	1.49—1.53
	62	0.67	3.89—3.96	1.49—1.55	0.00—0.05	1.41—1.53
$f_2(2010)$	53	0.66—0.67	3.42—4.35	1.04—1.18	0.00	0.54—0.70
	62	0.67	3.94—4.18	1.12—1.15	0.00	0.62—0.65

(a) We see from Table 1 that the partial decay widths of all the f_2 mesons are extremely narrow. Furthermore, $g_3 \ll g_1$, indicating the f-wave ($L=3$) component of the vertex is negligeable. Both are the consequence of the fact that the masses of these mesons are very close to the $p\bar{p}$ threshold. The narrowness of the partial width indicates that the $p\bar{p}$ decay channel must be a small part of the total decay of these f_2 mesons.

(b) The BES collaboration reported similar branching ration (BR) for $\xi \to p\bar{p}$, K^+K^-, $K_s^0K_s^0$, $\pi^+\pi^-$ decay modes. In subsequent publications[34,35] the BES collaboration reported the observation of $\xi \to \pi^0\pi^0$, $\eta\eta$, $\eta\eta'$, $\eta'\eta'$. It is indicated that the BR for $\pi^0\pi^0$ is similar to that for $\pi^+\pi^-$. However, in Ref.[34] the width Γ_ξ^{tot} was not given by the analysis but was prefixed at 20MeV. As to the BR for $\eta\eta$, $\eta\eta'$, $\eta'\eta'$, a much higher upper bound was given[35]. Assuming equal BRs for all these 8 decay modes and taking from Table 1 the average value of $\Gamma_{\xi\to p\bar{p}} = 1.94$MeV, we obtain a $\Gamma_\xi^{tot} \approx 16$MeV. Taking into account the experimental uncertainties of the widths given in Ref.[30], this 16MeV width represents already the observed value, implying there are no other decay modes left unobserved. This is a very unlikely possibility.

It was also reported in Ref.[30] that the BR of ξ decaying into $\pi^+\pi^-$ is equal to or less than 2 %. Assuming again equal BR, then the 2 %-fraction and $\Gamma_{\xi\to p\bar{p}} = 1.94$MeV imply that $\Gamma_\xi^{tot} = 1.94/0.02 = 97$MeV which is very large compared with the ~ 20MeV given in Ref.[30]. In order to obtain 20MeV, the 2 %-fraction would require the predicted $\Gamma_{\xi\to p\bar{p}}$ be reduced by a factor of 5, i.e., reducing the coupling constant g_1 by a factor of $\sqrt{5}$. We could not find such a solution in our analysis. Referring to Fig.1, one can see that at $s = 2800$ to 3600 $(\text{GeV})^2$, the pomeron exchange is already a good description of the data. This led us to believe that the uncertainty of the prediction, as could arise from assuming the pomeron exchange alone, cannot be as big as a factor of five. Consequently, we believe that the currently reported Γ_ξ^{tot} ($= 22 \pm 8$MeV)[4] is most likely an underestimate.

(c) A broad width is also consistent with the non-observation of a resonance structure in the 2.23GeV region in $\bar{p}p$ experiments[31]. We recall that there are many broad resonances in the neighborhood of 2.23GeV. Consequently, to $\bar{p}p$ reaction cross section is given by

$$\left(\frac{d\sigma}{dt}\right)_{a'a} \quad \sum_j \frac{c_{a'j}c_{ja}f(t)}{s - M_j^2 + iM_j\Gamma_j^{tot}}\Bigg|^2, \qquad (3)$$

where s and t are the total energy and the momentum transfer, $f(t)$ the t-dependence of the differential cross section. The indices a and a′ denote, respectively, the initial ($\bar{p}p$) and the final ($\bar{h}h$) channels, with $c_{ja} \propto \Gamma_{j\to a}^{1/2}$ and $c_{a'j} \propto \Gamma_{j\to a'}^{1/2}$ being the coupling of the initial and final states to the resonance j. Clearly, a resonance structure will not show up in the energy dependence of the cross section if $c_{ja} = 0$, i.e., if the resonance j does not exist. However, we advocate that even if the resonance does exist the structure may still not be seen in the data.

We have examined the general feature of the energy dependence of the $\bar{p}p \to h\bar{h}$ reaction by firstly considering the case where only one single resonance, the $f_2(2220)/\xi$, contributes. Our calculations have shown that the shape of this energy dependence is very senstive to the value of the Γ_ξ^{tot}. A resonance peak can be clearly seen in the mass region 2200 to 2500MeV when Γ_ξ^{tot} is narrower than 50MeV. However, the peak is no longer significant when Γ_ξ^{tot} is 75MeV, and disappears when Γ_ξ^{tot} reaches ~ 100MeV. This last value is in line with the 97MeV mentioned in (b). We have also noted that including other resonances in the calculation led to a futher reduction of the peak-to-background ratio but left the above main feature unaltered.

The $\bar{p}p$ experiment of Ref.[31] only scanned the mass region 2222.7 to 2239.7MeV. Consequently, that experiment can only confirm the existence of a narrow $f_2(2220)/\xi$ resonance. In other words, a non-observation of the resonance structure is not a sufficient ground for rejecting the existence of ξ, as it may just indicate that ξ has a broad width. Our analysis puts, therefore, a lower bound of about 100MeV for Γ_ξ^{tot}.

(d) It is generally accepted that the total decay width of a tensor glueball is narrow. However, current theoretical methods are still incapable of giving a quantitative statement about this narrowness. It is unclear whether 100MeV is too broad for a glueball.

5 Conclusions

The lightest particle that can be the soft pomeron

must have a spin of 2 and a mass in the 2.2GeV region. Three isoscalar tensor mesons, $f_2(2010)$, $f_2(2150)$, and $f_2(2220)/\xi$, fit this requirement. Regge analysis can predict the $f_2 \to p\bar{p}$ partial decay width which, when used in combination with the experimental branching ratios, can deterimine the total decay width of the meson. Comparison between the theroretical and experimental total widths will pin down the pomeron.

There is a great deal of interest in the $f_J(2220)/\xi$ meson because the reported[30] flavor-symmetry decay and narrow width of this meson fit what one expects from a glueball decay. However, the experimental situation is far from being settled. In particular, the ξ was not seen in $\bar{p}p \to \pi^0\pi^0$, $\eta\eta$ experiments. Our interest in the ξ is related to the search for pomeron, as this meson, with spin 2, is situated on the pomeron trajectory (cf. Fig.1). Our analysis has shown that the ξ must have a width much broader than the reported 22MeV. A broader width does not necessarily rule out the ξ as a glueball, but it does explain why the meson cannot be seen in the $\bar{p}p$ experiments.

We have noted there are other tensor states that satisfy the pomeron trajectory, among others, the $f_2(2150)$ and $f_2(2010)$ mesons. However, good experimental information about their decays to the $p\bar{p}$ channel is sparse. Better information on the branching ratios of their various decay modes will allow analyses be carried out at the same level as for the ξ.

If the spin of $f_J(2220)/\xi$ is confirmed to be 2 and if the improved measurement gives a width compatible with what has been inferred from our pomeron analysis, then the ξ can be identified with the pomeron. In this case, the pomeron will be a tensor glueball or at least have a dominant tensor glueball component. It is, however, still of great interest to carry out more detailed experimental studies of the $f_2(2150)$ and $f_2(2010)$ mesons as well as more refined theoretical studies on the gluonic content of their wave functions. By comparing the decay branching ratios of these two mesons with those of the ξ, one would better understand the pomeron.

Finally, we note that other diffractive processes where the pomeron exchange is believed to be dominant, such as diffractive dissociation of hadrons, electroproduction of vector mesons from the proton, virtual Compton scattering, etc., should also be used to improve our understanding of the soft pomeron and tensor states.

References

1 Regge T. Nuovo Cimento, 1959, **14**:951—960; **18**:947—961

2 Collins P D B. An Introduction to Regge Theory and High Energy Physics, Cambridge, Cambridge University Press, 1977. 1—99

3 Okum L B, Pomeranchuk I Y. Sov. Phys., 1956, 3:306—314; Okum L B, Pomeranchuk I Y. Sov. Phys., 1967, **JETP3**:307—340

4 Groom D E, Aguilar-Benitez M, Amsler et al. Review of Particle Physics, Euro. Phys., 2000, **J15**:233—235

5 Forshaw J R, Ross D A. Quantum Chromodynamics and The Pomerom, Cambridge, Cambridge University Press, 1977, 12—96

6 Jaroszkiewicz G A, Landshoff P V. Phys. Rev., 1974, **D10**:170—182; Donnachie A, Landshoff P V. Phys. Lett., 1983, **B123**:345—362

7 The uncertainties were not given in the original articles and the results of refitting the same inputs by us.

8 Block M A, Kang K, White A R. Int'l J. Mod. Phys., 1992, **A7**:4449—4459

9 More precisely, the relation is $\sigma^2_{tot}(s)/\sigma_{el}(s) = 16\pi(b + 2\alpha' \ln(s))/(1 + \rho^2)$ with ρ being the ratio of the real to imaginary parts of the forward amplitude. However, in the energy region of interest, $(\rho^2 + 1) \approx 1$

10 Engene J, Kooijman P. Prog. Part. Nucl. Phys., 1998, **41**:1—20

11 Laget J M, Galain R M Nucl. Phys., 1995, **A581**:397—406

12 Landshoff P V, Nachtmann O. Z. Phys., 1987, **C35**:405—416

13 Low F E. Phys. Rev., 1975, **D12**:163—176

14 Nussinov S. Phys. Rev. lett., 1975, **34**:163—176

15 Fadin V, Kuraev E A, Lipatov L N. Sov. Phys. 1977, **JETP45**:199—224; Balitxky Y Y, Lipatov L N. Sov. J. nucl. Phys., 1978, **28**:822—834

16 Dokshitzer Y L. Sov. Phys. 1977, **JETP73**:1216—1229; Gribov V N, Lipatov L N. Soc. J. Nucl., 1978, **15**:72—81; Altarelli G Parisi G. Nucl. Phys., 1977, **B126**:298—312

17 Collin J M, Peardon M. Phys. Rev., 1999, **D60**:034509—034560

18 Adam S, Swanson E S, Ji C R, Stephen R C. Phys. Rev. Lett., 1996, **76**:2011—2026

19 Kisslinger L S, MA Wei-Xing. Phys. Lett., 2000, **B485**:367—371

20 Close F E, Glennys F R, Li Z P. Phys. Rev., 1997, **D55**:5749—5760

21 Levin E. 25 years with the Pomeron, Aug. 1998, DESY 98—118, TAUP2521/98, hep-ph/9808483, 31 Aug. 1998

22 Michael C. AIP Conference Proc., 1997, **432**:657—682

23 Burakovsky L. Phys. Rev., 1998, **D58**:057503—057521

24 Close F E. Preprint, hep-hp/9701290 at XXX. lanl.gov

25 Burakovsky L, Page P R. Euro. Phys. J., 2000, **C12**:480—496

26 Baltkusaitis R M. Phys. Rev. Lett., 1986, **56**:107—114

27 Alde D M. Phys. Lett., 1986, **B177**:120—126

28 Aston D. Phys. Lett., 1988, **B215**:199—204

29 Breitweg J. DESY 98—107; Abatzis S. Phys. Lett., 1994, **B324**: 509—514

30 BAI J Z. Phys. Rev. Lett., 1996, **76**:3502—3510

31 Seth K K. Nucl. Phys., 2000, **A675**:25—35c

32 Predazzi E. Diffraction: Past, Present and Future. 1999, Preprint, INFEN, Sezione di Torino, 10125 Torino, Italy

33 LIU L C, MA W X. J. Phys., 2000, **G26**:159—64

34 BAI J Z. Phys. Rev. Lett., 1998, **81**:1179—1184

35 SHEN X. in Hadron Spectroscopy, ed. By Chung S U, Willutzki H, AIP Conf. Proc. 1998, **432**:47—60

36 Jacob M, Wick G C. Ann. Phys. (N. Y.), 1959, **7**:404—456

37 Haider Q, LIU L C. J. Phys., 1996, **G22**:1187—1198

38 Martin A D, Spearman T D. Elementary Particle Theory, North-Holland Publ. Co. -Amsterdam and John Wiley & Sons, Inc. -New York, 1970, 46—89

Appendix

Pomeron Analysis With a Singularity-free Form Factor

We recapitulate the key results of Ref. [33]. The standard definition of the Mandelstam variables, helicities, and residue functions are employed. The t-channel Regge amplitude in the helicity basis[36] is

$$A^{(t)}_{\lambda_{\bar 2}\lambda_4;\lambda_1\lambda_{\bar 3}}(\bar s,t) = C_t\,\frac{-4\pi^2(2\alpha+1)\beta_{\lambda\lambda'}(t)(-1)^{\alpha+\lambda}\,\frac{1}{2}[1+(-1)^{\alpha}]}{\sin\pi(\alpha+\lambda')}\,d^{\alpha}_{\lambda\lambda'}(z_t), \tag{A1}$$

where $C_t = 1/2$, $s = t$, $\bar t = s$. The $\beta_{\lambda\lambda'}(t) \equiv \beta_{\lambda_{\bar 2}\lambda_4;\lambda_1\lambda_{\bar 3}}(\bar s)$ is the Regge residue. The λ_i is the helicity of the particle i, and $\alpha \equiv \alpha(t)$ is the trajectory spin. In Eq. (A1), we have introduced for clarity the variables $\bar s$ and $\bar t$ which denote, respectively, the total c.m. energy and the momentum transfer in the t-channel.

On the other hand, the Feynman amplitude due to exchanging a meson of spin J_2 is

$$A^{(s)}_{\lambda_{\bar 2}\lambda_4;\lambda_1\lambda_{\bar 3}}(t,s) = -4M_p^2\,\frac{4\pi(2J_2+1)}{2}\langle\lambda_{\bar 2}\lambda_4|\mathscr{M}^{J_2}(t)|\lambda_1\lambda_{\bar 3}\rangle\,d^{J_2}_{\lambda\lambda'}(z_t), \tag{A2}$$

with

$$\langle\lambda_{\bar 2}\lambda_4|\mathscr{M}^{J_2}(t)|\lambda_1\lambda_{\bar 3}\rangle = \frac{G_\lambda H^{J_2}_{\lambda_{\bar 2}\lambda_4}(t)\,G_{\lambda'}H^{J_2}_{\lambda_1\lambda_{\bar 3}}(t)}{t - M^2_{f_2} + iM_{f_2}\Gamma^{tot}_{f_2}}. \tag{A3}$$

In Eq. (A3), $J_2 = 2$, $\lambda \equiv \lambda_1 - \lambda_{\bar 3}$, and $\lambda' \equiv \lambda_{\bar 2} - \lambda_4$. The $H(t)$ denotes the form factor of the $p\bar p f_2$ vertex in the helicity basis with G being the coupling constant, and M_{f_2}, $\Gamma^{tot}_{f_2}$, respectively, the mass and the full (total) decay width of the f_2 meson.

The reggeization of f_2-exchange was realized through projecting the discrete spin value J_2 onto the continuous spin value α of the Regge trajectory and the result is[33]

$$\beta_{\lambda\lambda'}(t) = \alpha'_R 4M_p^2\,G_{\lambda'}H_{\lambda_{\bar 2}\lambda_4;J_2}(t)\,G_\lambda H_{J_2;\lambda_1\lambda_{\bar 3}}(t), \tag{A4}$$

where $\alpha'_R \equiv \mathrm{Re}[\alpha']$. Eq. (A4) gives a Feynman description of the residue factorization used extensively in the Regge theory, which also answers why we started with the t-channel amplitude. We may also notice that the factorization of the Regge residue β is achieved at the same time of the reggeization

The GH is directly related to the partial decay width $\Gamma_{f_2\to p\bar p}$ through[37]

$$\frac{1}{2}\Gamma_{f_2\to p\bar p} = \mathrm{Im}[\Pi_{f_2}(t)] = C_t\,\frac{M_p^2}{M_{f_2}^2}\,\frac{|\boldsymbol{q}_r|}{16\pi^2}\sum_{\lambda_p\lambda_{\bar p}}|G_\lambda H_{\lambda_p\lambda_{\bar p};J_2}(q_r^2)|^2$$

where $\boldsymbol{q}_r^2 \equiv t_r/4 - M_p^2 \equiv M_{f_2}^2/4 - M_p^2$ and $\lambda = \lambda_p - \lambda_{\bar p}$. The $\boldsymbol{q}_r$ is the on-shell $p\bar p$ relative momentum in the c.m. of the meson. Eq. (A5) shows that the vertex GH can be obtained from calculating the self-energy $\Pi_{f_2}(t)$ of the tensor state. Conversely, one can determine GH from pp scattering and to use it to predict $\Gamma_{f_2\to p\bar p}$.

The s-channel amplitude is obtained through crossing-symmetry which reads

$$A^{(s)}_{(pp\to pp);\lambda_3\lambda_4;\lambda_1\lambda_2} = U_{\lambda_3\lambda_4\lambda_1\lambda_2;\lambda_{\bar 2}\lambda'_4\lambda'_1\lambda_{\bar 3}}\,A^{(t)}_{(p\bar p\to\bar p p);\lambda_{\bar 2}\lambda'_4;\lambda'_1\lambda_{\bar 3}}. \tag{A6}$$

Since there are five independent helicity amplitudes, U is a 5×5 unitary matrix[38]. The cross sections are given by[33]

$$\sigma^{pp}_{tot} = \frac{1}{2s}\sum_{\lambda_3\lambda_4;\lambda_1\lambda_2}\mathrm{Im}\left[A^{(s)}_{\lambda_3\lambda_4;\lambda_1\lambda_2}\right]_{t=0} = \frac{1}{2s}\mathrm{Im}\left[4A_1^{(t)} + 8A_5^{(t)}\right]_{t=0},$$

and

$$\frac{d\sigma^{pp}}{dt} = \frac{1}{16\pi s^2}\sum_{\lambda_3\lambda_4;\lambda_1\lambda_2}\left|A^{(s)}_{\lambda_3\lambda_4;\lambda_1\lambda_2}\right|^2 = \frac{1}{16\pi s^2}(4|A_1^{(t)}|^2 + 4|A_3^{(t)}|^2 + 8|A_5^{(t)}|^2). \tag{A8}$$

In the above equations, $A_i^{(t)}(i = 1,2,3)$ are three of the five independent helicity amplitudes corresponding respectively to $(\lambda_{\bar 2}\lambda_4;\ \lambda_1\lambda_{\bar 3}) = (++,\ ++)$, $(+-;\ +-)$, $(++;\ +-)$. The second equality in Eqs. (A7) and (A8) is due to crossing symmetry properties of the amplitudes.

It is advantageous to model the form factor H in the LS-basis because in this latter basis the form factor has a well-known $|\boldsymbol{q}|^L$ threshold behavior that can be explicitly incorporated into the model. The helicity basis is related to the LS-basis by a unitary transformation[36]. Hence,

$$\sum_\lambda|G_\lambda H_{\lambda_p\lambda_{\bar p};J_2}(t)|^2 = \sum_{LS}|g_{LS}F_{LS}(t)|^2 \tag{A9}$$

where F_{LS} and g_{LS} denote, respectively, the form factor and the coupling constant in the LS basis. For the $p\bar{p}$ system with $J^{PC} = 2^{++}$, the parity conservation leads to $L = 1, 3$ and $S = 1$ only. If the form factor is defined in such a way that $F_{LS}(t_r) = 1$, then

$$\Gamma_{\xi\to p\bar{p}} = C_I \frac{M_p^2}{M_{f_2}^2} \frac{|q_r|}{16\pi^2}(g_{L=1,S=1}^2 + g_{L=3,S=1}^2). \quad (A10)$$

Because there is only one value of S, the label S will be dropped but understood in what follows.

It is important to use a form factor which is analytic in both the direct and crossed channels. Liu and Ma proposed the following singularity-free form factor[33]:

$$(F_L(t))^2 = \left(\frac{t/4 - M_p^2}{t_r/4 - M_p^2}\right)^L \left(\frac{e^{t_r/\lambda_t^2}}{R(-x_t) + e^{t/\lambda_t^2}}\right)^2 \left(\frac{1 + e^{-t_r/\lambda_s^2}}{R(x_s) + e^{-t/\lambda_s^2}}\right)^2 \quad (A11)$$

where the first factor on the r.h.s. is equal to (q^{2L}/q_r^{2L}). Here, q and q_r are, respectively, the off- and on-shell $p\bar{p}$ relative momentum in the c.m. of the f_2 meson. The F_L has, therefore, the correct threshold q^L-dependence. In Eq.(A11), the λ_s, λ_t are the ranges of the form factor, $x_s \equiv (t - 2M_p^2)/\lambda_s^2$, and $x_t \equiv (t - 2M_p^2)/\lambda_t^2$. The function R is defined by

$$R(x) = \frac{1}{2}(1 + \tanh(ax)) = \frac{e^{ax}}{e^{ax} + e^{-ax}}, \quad (A12)$$

which is analytic and varies rapidly from 0 to 1 when x changes from $x < 0$ to $x > 0$, with a controling the transition speed at $x = 0$. With $a > 10$, R will be very close to a step function but does not have the discontinuity of the latter. In fact, R and F_L are infinitely differentiable.

The above analytic property is absent in the commonly used hadronic form factors in the literature, which are either of an exponential form or of a multipole form. We emphasize that these conventional form factors are unsuitable to analyses involving channel-crossing. For example, the exponential form factor $\exp(t/\Lambda^2)$ is analytic in the s-channel where $t \leqslant 0$ but diverges in the t-channel where $t > 0$. The multipole form factor $[\Lambda^2/(\Lambda^2 - t)]^n (n = 1, 2, \cdots)$ has no pole on the real axis of t in the s-channel (where $t \leqslant 0$) but will have it in the t-channel (where $t > 0$). Conversely, if we use $\exp(-t/\Lambda^2)$ or $[\Lambda^2/(\Lambda^2 + t)]^n$, then the situation will be reversed.

The form factor of Eq.(A11) does not have these singularities. In the physical domain of the t-channel (i.e., $t > 4M_p^2$),

$$(F(t))^2 \propto \frac{q^{2L}}{(e^{t/\lambda_t^2})^2(1 + e^{-t/\lambda_s^2})^2} \xrightarrow{t\to+\infty} \frac{t^L}{e^{2t/\lambda_t^2}} \quad (A13)$$

which goes to zero, exhibiting the correct energy behavior in the t-channel. We can see that in the t-channel the λ_t controls the form factor. In the s-channel, $t \leqslant 0$. Hence, $R(-x_t) \approx 1$ and $R(x_s) \approx 0$. It follows that

$$(F(t))^2 \propto \frac{q^{2L}}{(1 + e^{t/\lambda_t^2})^2(e^{-t/\lambda_s^2})^2} \xrightarrow{t\to-\infty} \frac{t^L}{e^{-2t/\lambda_s^2}}. \quad (A14)$$

Hence, λ_s controls the form factor in the s-channel. This singularity-free form factor satisfies the analyticity requirement of the Regge theory and can be used for making analytical continuation between direct and crossed channels. Two remarks are in order.

(a) Eq.(A3) is given for the sole purpose of making the connection between the t-channel Regge and Feynman amplitudes. It is not needed in fitting the pp scattering data. Hence, the width $\Gamma_{f_2}^{tot}$ is not an input to the Regge analysis in Ref.[33]. As to the mass M_{f_2}, it enters the analysis through the quantity $t_r (\equiv M_{f_2}^2)$ in the form factor, which amounts to a redefinition of the normalization factor and is, therefore, also not an input of dynamics.

(b) The important physics inputs are the spin of the meson, J_2, which determines the values of L in the form factor $F_L(t)$, and the property of the pomeron trajectory.

Eqs. (A1), (A4), (A7), (A8), and (A11) were used to fit the pp total and elastic differential cross sections simultaneously. The results are given in Table 1.

关于软坡密子的张量胶子球的内涵

周丽娟[1;1)]　马维兴[1,2]　刘龙章[3]

1(广西工学院信息与计算科学系　柳州　545006)

2(中国科学院高能物理研究所　北京　100039)

3(美国洛斯阿拉莫斯国家实验室理论部　T-16　新墨西哥州　87545)

摘要　通过把坡密子的轨迹跟观察到的量子数 $I^G J^{PC} = 0^+ 2^{++}$ 的同位旋标量的张量介子联系起来的关系,研究了坡密子的胶子球内涵.这些介子中有四个满足坡密子的自旋和质量的关系.这些坡密子的后选者可能是混合态.其中,$f_2(2220)$有极大的胶子球分量.讨论了关于这个介子宽度的实验争论,预言了它的理论下限,也阐明了在 pp 实验研究中观察不到 $f_2(2220)$原因.

关键词　坡密子　胶子球　介子

2003 - 03 - 10 收稿

* 国家自然科学基金(10247004,10075081)资助

1) E-mail:MAWX@mail.ihep.ac.cn